Article

Cell Reports

MCT4 Defines a Glycolytic Subtype of Pancreatic Cancer with Poor Prognosis and Unique Metabolic Dependencies

Graphical Abstract

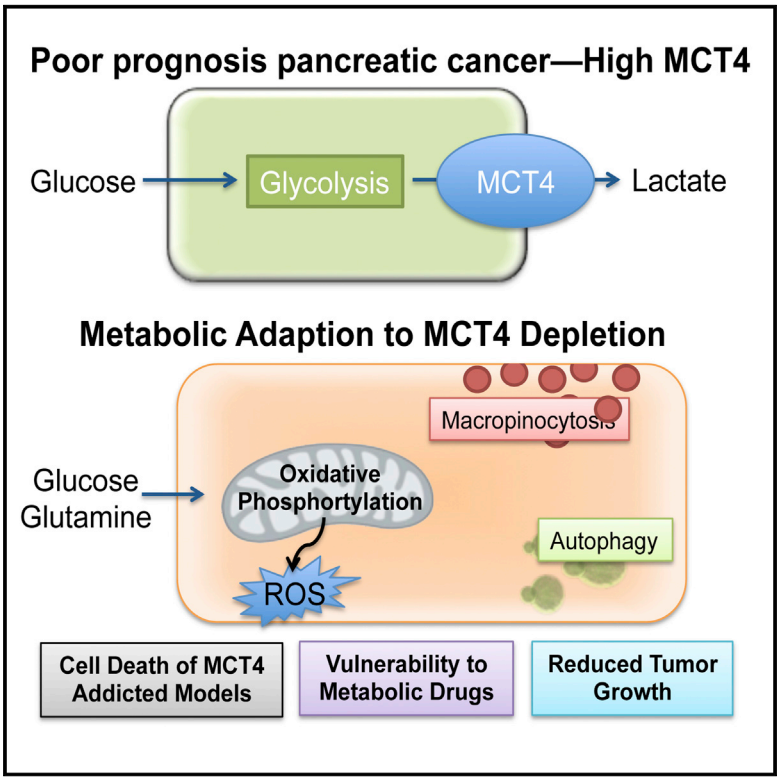

Authors

GuemHee Baek, Yan F. Tse, ..., Erik S. Knudsen, Agnieszka K. Witkiewicz

Correspondence

agnes.witkiewicz@utsouthwestern.edu

In Brief

In pancreatic cancer, many metabolic features are driven by KRAS mutation. Baek et al. report that the lactate transporter MCT4 is a critical determinant of disease prognosis and glycolytic metabolism. These findings demonstrate distinct metabolic subtypes of pancreatic cancer and delineate metabolic vulnerabilities associated with lactate export.

Highlights

- MCT4 is associated with glycolytic metabolism and poor-prognosis pancreatic cancer
- In addicted models, MCT4 is required for maintenance of effective metabolic activity
- Depletion of MCT4 induces compensatory metabolism to avert a metabolic crisis
- Targeting MCT4 suppresses tumor growth and yields vulnerability to metabolic stress

Accession Numbers

GSE63231

Baek et al., 2014, Cell Reports 9, 2233–2249
December 24, 2014 ©2014 The Authors
http://dx.doi.org/10.1016/j.celrep.2014.11.025

Cell Reports
Article

MCT4 Defines a Glycolytic Subtype of Pancreatic Cancer with Poor Prognosis and Unique Metabolic Dependencies

GuemHee Baek,[1] Yan F. Tse,[1] Zeping Hu,[3] Derek Cox,[1] Noah Buboltz,[4] Peter McCue,[4] Charles J. Yeo,[5] Michael A. White,[6] Ralph J. DeBerardinis,[2,3] Erik S. Knudsen,[1,2] and Agnieszka K. Witkiewicz[1,2,*]
[1]Department of Pathology, UT Southwestern, Dallas, TX 75390, USA
[2]Simmons Cancer Center, UT Southwestern, Dallas, TX 75390, USA
[3]Children's Medical Center Research Institute at UT Southwestern, Dallas, TX 75390, USA
[4]Department of Surgery, Thomas Jefferson University, Philadelphia, PA 19107, USA
[5]Department of Pathology, Thomas Jefferson University, Philadelphia, PA 19107, USA
[6]Department of Cell Biology, UT Southwestern, Dallas, TX 75390, USA
*Correspondence: agnes.witkiewicz@utsouthwestern.edu
http://dx.doi.org/10.1016/j.celrep.2014.11.025

SUMMARY

KRAS mutation, which occurs in ~95% of pancreatic ductal adenocarcinoma (PDA), has been shown to program tumor metabolism. MCT4 is highly upregulated in a subset of PDA with a glycolytic gene expression program and poor survival. Models with high levels of MCT4 preferentially employ glycolytic metabolism. Selectively in such "addicted" models, MCT4 attenuation compromised glycolytic flux with compensatory induction of oxidative phosphorylation and scavenging of metabolites by macropinocytosis and autophagy. In spite of these adaptations, MCT4 depletion induced cell death characterized by elevated reactive oxygen species and metabolic crisis. Cell death induced by MCT4-depletion was augmented by inhibition of compensatory pathways. In xenograft models, MCT4 had a significant impact on tumor metabolism and was required for rapid tumor growth. Together, these findings illustrate the metabolic diversity of PDA described by MCT4, delineate pathways through which this lactate transporter supports cancer growth, and demonstrate that PDA can be rationally targeted based on metabolic addictions.

INTRODUCTION

Pancreatic ductal adenocarcinoma (PDA) has a particularly poor prognosis, and even with new targeted therapies and chemotherapy, the 5-year survival rate of pancreatic cancer is ~6% (Bardeesy and DePinho, 2002; Hezel et al., 2006; Wolfgang et al., 2013; Wood and Hruban, 2012). Due to this recalcitrance to therapy, it is important to understand the biology of PDA and identify putative therapeutic targets beyond the current focus on chemotherapy or therapies directed at deregulated oncogenic pathways (Almhanna and Philip, 2011). One of the key challenges in the treatment of pancreatic cancer is the lack of defined subtypes of disease to which therapy should be directed (Tempero et al., 2013), and therefore, unlike other cancers, PDA is treated largely as a single disease type.

One of the emerging and provocative therapeutic approaches is to target specific metabolic dependencies of cancer (Cheong et al., 2012; Deberardinis et al., 2008; Le et al., 2012; White, 2013). PDA exhibits the presence of abundant desmoplastic stroma, which accounts for the majority of tumor volume (Chu et al., 2007; Erkan et al., 2012). Dense fibrotic stroma in connection with poor vascularization results in a hypoxic and acidic microenvironment (Brahimi-Horn et al., 2011; Ide et al., 2007; Neesse et al., 2011). This environment and the presence of activated KRAS are believed to promote a reprogramming of metabolism within tumor cells to favor glycolysis. However, it is clear that the metabolic features of disease are complex, and PDA is known to utilize multiple independent processes and nutrients for energy and to provide precursors of proteins, nucleic acids, and membrane lipids (Le et al., 2012; Son et al., 2013). Additionally, PDA has been described to exhibit high levels of autophagy and macropinocytosis to ostensibly scavenge macromolecules to fuel tumor cell proliferation and enable survival under stress conditions (Commisso et al., 2013; Yang and Kimmelman, 2011; Yang et al., 2011). The complex flow of nutrient sources into the tumor cells suggests that targeting common aspects of the efflux of metabolic waste may represent a particularly important feature of PDA (Parks et al., 2013).

Many cancer cells activate aerobic glycolysis and convert the majority of glucose into lactate, even when oxygen is available for oxidative phosphorylation (Halestrap and Price, 1999; Halestrap and Wilson, 2012). To survive the accumulation of lactate and maintain an intracellular acid-base balance, cancer cells acquire proton pumps, sodium-proton exchangers, bicarbonate transporters, and monocarboxylate transporters (MCTs). MCTs are transmembrane proteins that facilitate the transport of short-chain carbohydrates such as pyruvate and lactate, with

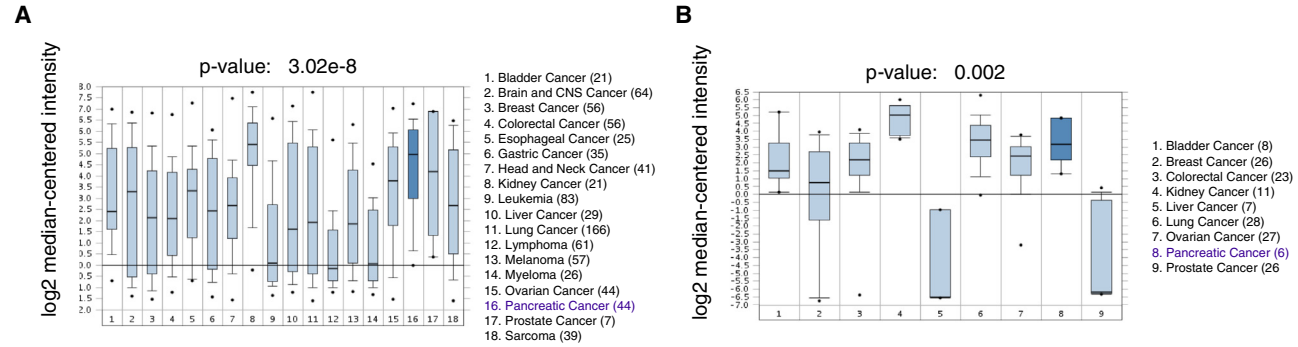

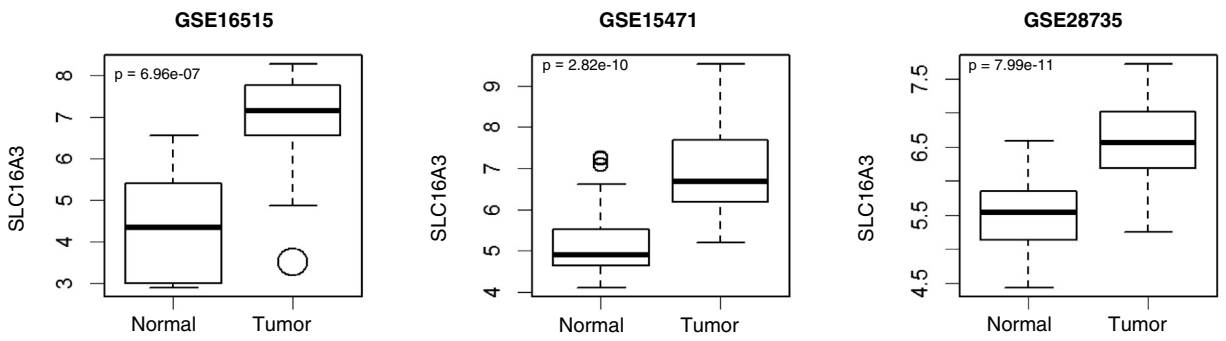

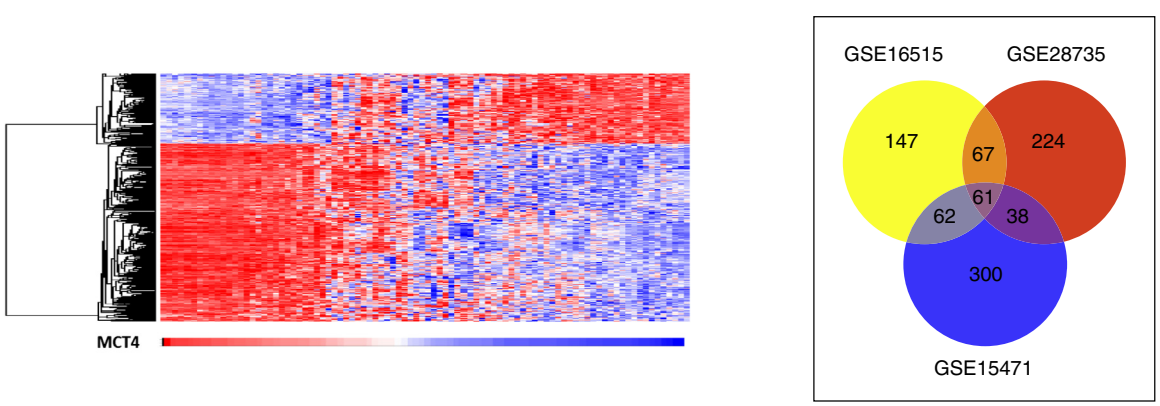

E

Term	p-Value	Fold Enrichment	Bonferroni
collagen fibril organization	1.10e-06	19.75112444	8.30e-04
glycolysis	1.43e-06	13.92784459	0.001077125
monosaccharide catabolic process	2.37e-05	9.219840784	0.017697654
cellular carbohydrate catabolic process	7.63e-05	7.701278772	0.055880152

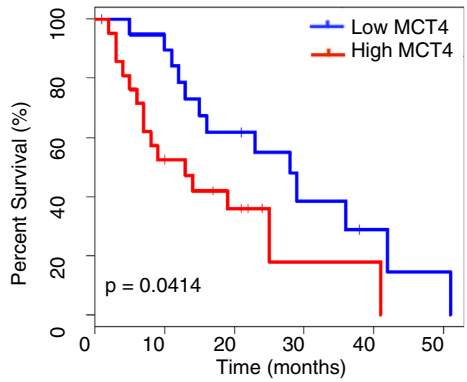

(legend on next page)

MCT1–MCT4 being preferentially involved in the transport of lactic acid (Halestrap, 2012; Halestrap and Meredith, 2004; Pinheiro et al., 2012). Export of lactate by MCTs prevents a decrease in cytosolic pH and inhibition of continued glycolysis (Draoui and Feron, 2011; Halestrap and Wilson, 2012; Parks et al., 2013). MCT1 has relatively ubiquitous tissue expression and plays a role in lactate shuttle in the heart, slow-twitch skeletal muscle, red blood cells, and the liver. Other MCT proteins demonstrate more tissue-specific expression, with MCT2 being present in neurons and MCT3 being limited to retinal pigmented epithelium and choroid plexus epithelium (Philp et al., 2001). MCT4 is restricted to "glycolytic" tissues such as rapid-twitch skeletal muscle and astrocytes (Bergersen et al., 1999; Bergersen, 2007; Bonen, 2000; Halestrap, 2012; Halestrap and Wilson, 2012). Given their central role in controlling intracellular pH and lactate-based metabolism, MCT1 and MCT4 have been evaluated in various cancers, including cervical (Pinheiro et al., 2008), colorectal (Pinheiro et al., 2008), breast (Pinheiro et al., 2010; Whitaker-Menezes et al., 2011), melanoma (Su et al., 2009), kidney (Gerlinger et al., 2012), and lung (Pinheiro et al., 2010) cancers. In general, the upregulation of MCT proteins is observed in tumor tissue and supports an apparent need for lactate shuttling to either fuel tumor growth or enable survival under stress conditions (Parks et al., 2013).

There is an increasing interest in targeting lactate transporters in cancer. Much of the emphasis has been on MCT1, which is generally viewed as playing a pivotal role in lactate influx to facilitate mitochondrial metabolism (Doherty et al., 2014; Polański et al., 2014; Sonveaux et al., 2012), or CD147, which is a required scaffolding protein for both MCT1 and MCT4 (Le Floch et al., 2011; Schneiderhan et al., 2009). Drugs that selectively block lactate influx through MCT1 have been shown to impact tumor cell growth and survival (Draoui et al., 2014), although MCT1 inhibition can also block efflux of lactate (Doherty et al., 2014). Functional studies have shown that the inhibition of specific lactate transporters can result in disparate effects on tumor cell proliferation and viability depending on the model used, the nature of the targeted transporter, and the methodology employed to measure the impact on metabolism (Doherty et al., 2014; Gerlinger et al., 2012; Le Floch et al., 2011; Lee et al., 2012; Polański et al., 2014; Schneiderhan et al., 2009; Sonveaux et al., 2012).

Here, we evaluated the expression of lactate transporters in PDA and observed a striking upregulation of the *Slc16A3* gene encoding MCT4. MCT4 expression was heterogeneous in PDA and associated with glycolytic metabolism and poor prognosis. This finding was confirmed by immunohistochemical analysis in a large cohort of pancreatic carcinoma cases, and the prognostic significance was retained in multivariate analysis. MCT4 depletion in "addicted" models resulted in a metabolic crisis that invoked compensatory mechanisms related to multiple metabolic pathways and nutrient-scavenging mechanisms. In spite of these adaptations, MCT4 depletion had a pronounced impact on cellular viability and tumorigenic growth that was further augmented by targeting of compensatory processes. Together, these data underscore the metabolic diversity of PDA, the key regulatory function of MCT4, and the intersecting roles of multiple metabolic processes in specifying tumor cell survival.

RESULTS

Expression of MCT1-4 in Pancreatic Cancer

Initially, the genes encoding the key lactate transporters MCT1–MCT4 were evaluated in PDA. Among these genes, only Scl16A1 (encoding MCT1) was elevated in tumor versus normal specimens (Figure S1). However, there was little overexpression of *Slc16A1* in PDA versus other cancers (Figure S1). In contrast, the levels of the *Slc16A3* transcript encoding MCT4 were high in PDA and comparable to those in renal clear cell carcinoma, which is known to express very high levels of MCT4 (Gerlinger et al., 2012). This was apparent in both cell lines (Figures 1A and S1) and tumor samples (Figures 1B and S1). In addition, *Slc16A3* expression was considerably higher in tumor specimens than in normal specimens (Figure 1C). To determine the gene-expression program associated with elevated *Slc16A3*, we identified genes with a high positive or negative correlation to *Slc16A3* from each of the data sets (Figure 1D). Genes that were common to two of the three data sets were employed as an "*Slc16A3*/MCT4 signature." Gene Ontology analysis demonstrated that high *Slc16A3* expression is associated with a gene-expression program involving collagen fibril organization and multiple aspects of glycolytic metabolism (Figure 1E). Although PDA generally has a poor prognosis, we evaluated the association of *Slc16A3* expression levels with overall survival in the data set that contained clinical follow-up information. Kaplan-Meier analysis showed that high *Slc16A3* was associated with poor outcome (Figure 1E). These data suggest that although *Slc16A3* is generally elevated in PDA, it also shows a diversity of expression that has prognostic and functional significance.

Coordinated MCT4 Expression in Tumor Epithelial and Stromal Compartments Is Associated with Particularly Poor Prognosis

To further explore the impact of MCT4 on PDA, we analyzed a cohort of 223 patients who had undergone surgical resection. Table S1 shows the descriptive statistics (age, tumor size, histologic grade, lymph-node status, stage, margin status, vital

Figure 1. MCT4 Expression Is Elevated in PDA

(A) Gene-expression analyses of *SLC16A3* in a panel of cancer cell lines demonstrated a statistically significant increase in expression in PDA versus 17 other cancer cell types.

(B) Gene-expression analyses of *SLC16A3* demonstrated significantly increased expression in pancreatic carcinoma versus eight other malignancies.

(C) Differential expression analyses demonstrated increased expression of *SLC16A3* in pancreatic carcinoma versus normal tissue.

(D) Hierarchical clustering of MCT4-correlated genes, and overlap among the three data sets.

(E) Top Gene Ontology categories associated with the MCT4 signature and their association with disease outcome.

See also Figure S1.

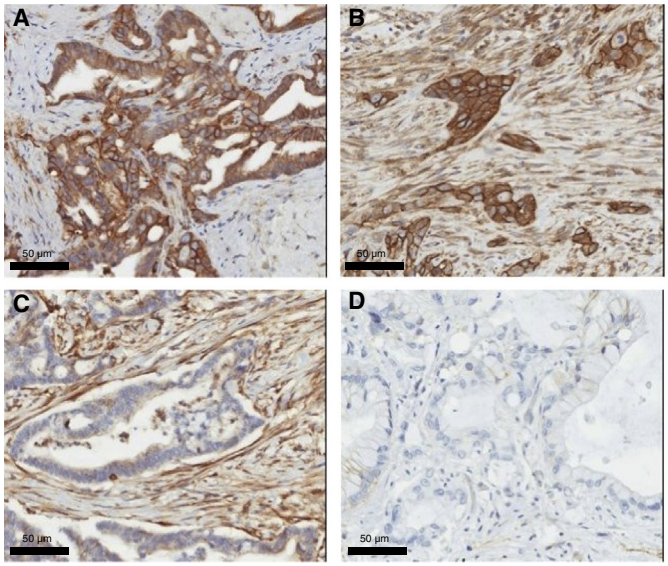

E

	MCT4 (EPITHELIA)	
MCT4 (STROMAL)	LOW	HIGH
LOW	71 (34.4)	65 (31.7)
HIGH	13 (6.4)	56 (27.3)

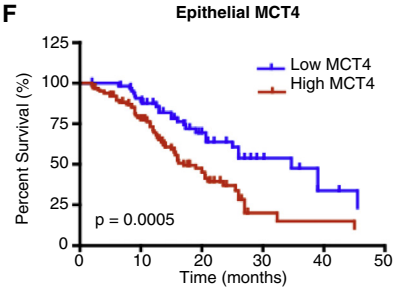

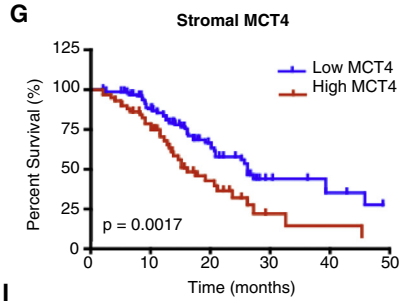

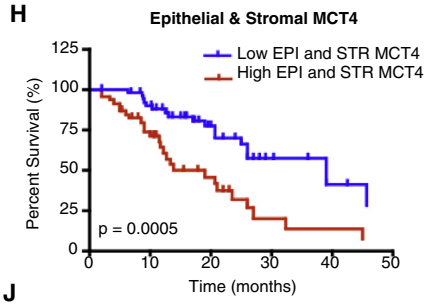

I

Univariate	P-Value	Hazard Ratio	95% CI
Grade	0.0017	1.67	1.03 - 2.305
Node Status	0.0546	1.902	1.29 - 2.52
MCT4 (epi)	0.0005	2.38	1.46 - 3.86
MCT4 (stroma)	0.0017	2.09	1.32 - 3.31
Combined (EPI+Stromal) MCT4	0.0005	2.74	1.64 - 5.80

J

	P value	Hazard Ratio	95% CI
Cox-multivariate			
Grade	0.1160	1.503	0.904 - 2.499
Node Status	0.0875	1.621	0.931 - 2.822
MCT4 (epi)	0.0015	2.264	1.365 - 3.756
Cox-multivariate			
Grade	0.0620	1.451	0.981 - 2.146
Node Status	0.3047	1.328	0.773 - 2.282
MCT4 (stroma)	0.0106	1.557	1.109 - 2.187

Figure 2. MCT4 Expression Is Associated with PDA Prognosis

(A–D) Representative images of immunohistochemical staining show high epithelial-specific staining (A), high stromal and epithelial staining (B), high stromal-specific staining (C), and low staining of MCT4 in PDA (D).

(E) Summary of compartment-specific expression in all cases.

(F) Kaplan-Meier analysis of epithelial MCT4 expression and overall survival.

(G) Kaplan-Meier analysis of stromal MCT4 expression and overall survival.

(H) Kaplan-Meier analysis of combined high epithelial and stromal MCT4 expression versus all other conditions.

(I) Univariate analysis of MCT4 staining in epithelial and stromal compartments.

(J) Cox multivariate analysis of MCT4 staining in epithelial and stromal compartments.

See also Figure S2 and Tables S1 and S2.

status, and treatment information) for the study patient population. Representative images of MCT4 immunohistochemical staining are depicted in Figures 2A–2D. MCT4 levels were high (panels A and B) or low (C and D) in the tumor compartment, and correspondingly high (panels B and C) or low (A and D) in the stromal compartment. As shown in Figure 2E, 121 cases had high MCT4 expression in the epithelial compartment, 69 cases had high MCT4 in the stromal compartment, and 56 cases displayed high expression in both compartments. Only 13 cases had high expression in the stroma and low expression within the tumor compartment. Thus, although all combinations could be found, cases with high stromal MCT4 were clearly associated with cases that exhibited high MCT4 staining within the tumor (Figure 2E). We evaluated both tumor and stromal MCT4 for association with survival. Kaplan-Meier analysis showed that tumors with high MCT4 expression in either the epithelial compartment or the stromal compartment had poor survival (Figures 2F and 2G). These findings were not a general feature of MCT expression, as expression of MCT1 was restricted to the epithelial compartment and was not associated with outcome (Figure S2). There was also no discrete association of MCT1 and MCT4 status in PDA specimens (Figure S2). Importantly, MCT4-related outcome data were statistically significant in univariate (Figure 2I) and multivariate models that incorporated tumor grade and lymph-node status (Figure 2J). We also evaluated the combined expression of epithelial and stromal MCT4 using Kaplan-Meier survival curves comparing cases that had strong MCT4 expression in both compartments versus all other cases (Figure 2H; Table S2). These data demonstrated that elevated expression of MCT4 is associated with particularly poor survival and suggest that elevated levels of MCT4 have a specific impact on the biology of PDA.

Differential Expression of MCT4 in Pancreatic Cancer Cell Lines

To characterize the function of MCT4 in PDA, we evaluated endogenous expression across cell lines. These analyses showed that the majority of PDA cell lines harbor high levels of MCT4, presumably indicating aggressive disease (Figure 3A). Consistent with this concept, cell lines that exhibit a "mesenchymal phenotype" and are vimentin positive, such as PL45 and Panc1, had higher expression of MCT4 than the "epithelial phenotype" Capan-2 line (Figure 3B). The expression of LDHA, which catalyzes the production of lactate from pyruvate, was largely elevated in pancreatic models, but did not correlate tightly with the status of MCT4 protein (Figure 3A). The basal protein expression was related to the relative levels of the MCT4 transcript, and, interestingly, in pancreatic cancer models, MCT4 was only modestly responsive to hypoxia (Figure S3). Since mutant KRAS has been invoked as a critical mediator of pancreatic cancer metabolism, we evaluated the association of KRAS mutation with MCT4 expression. Interestingly, MCT4 levels were not simply associated with KRAS mutation status, as PL5 harboring wild-type KRAS expressed higher levels of MCT4 than the mutant KRAS cell line Capan-2 (Figure 3C). Recognizing that there are likely multiple means by which KRAS signaling can be induced in lines with wild-type protein, we employed MEK inhibitors to define the importance of this key downstream pathway (Figure 3D). MEK inhibition resulted in the attenuation of MCT4 expression in all cell lines evaluated, with the exception of Capan-2, which showed low levels of endogenous MCT4, indicating that deregulated KRAS/MEK signaling is required for a high level of MCT4 expression. MEK suppression had a relatively weak effect on the transcript level of MCT4 (not shown); however, the use of the proteasome inhibitor could largely blunt the attenuation of protein levels with MEK inhibition (Figure S3). These data were also recapitulated when KRAS-specific RNAi was used (Figure 3E).

To determine whether MCT4 status was associated with a metabolic preference in culture, we monitored glycolytic metabolism by assessing the extracellular acidification rate (ECAR), which is a surrogate measure for lactate secretion as an end product of glycolysis. As shown in Figure 3F, PL45 and MIA PaCa-2, which express high levels of MCT4, exhibited substantial glycolytic activity. Interestingly, in these cells, the glycolytic function appeared to operate at close to maximum capacity, as indicated by the moderate effects of oligomycin. In contrast, Capan-2 cells did not substantively engage in glycolysis. Correspondingly, PL45 and MIA PaCa-2 cells were more sensitive to acute glucose withdrawal than Capan-2 cells (Figure 3G). These data indicate that MCT4 expression is a potent marker of glycolytic activity.

Inhibition of MCT4 Alters PDA Metabolism

In order to evaluate the functional significance of MCT4 in PDA, we performed acute knockdown across cell lines. The multiple siRNAs that were used produced consistent results in targeting MCT4, with a uniform impact on distal biological processes (Figure S3). The loss of membrane-associated MCT4 protein (as revealed by immunofluorescence) and loss of total protein (as revealed by immunoblot analysis) was demonstrated following RNAi-mediated knockdown (Figures 3H and 3I). Depletion of MCT4 did not affect the mesenchymal nature of these cells (as indicated by the continued expression of vimentin). MCT4 knockdown resulted in enhanced expression of MCT1, whereas CD147, which serves as a dimeric partner for both MCT1 and MCT4, was only modestly affected. The effect of MCT4 on MCT1 expression was not transcriptional (data not shown), but resulted in increased MCT1 localization at the plasma membrane (Figure S3). These findings are consistent with the established competition between MCT1 and MCT4 for CD147 binding and membrane trafficking (Halestrap, 2012; Kirk et al., 2000). Analysis of glycolysis under this condition demonstrated a significant suppression in both PL45 and MIA PaCa-2 cell lines, but almost no effect on Capan-2 cells (Figures 3J–3L). These findings suggest that endogenous high-MCT4 status delineates a metabolic subtype in which high levels of continued glycolytic activity are dependent on MCT4.

To directly evaluate the impact of MCT4 depletion on metabolism, we measured the consumption of glucose and subsequent secretion of lactate into the media (Figure 4A). These data demonstrated that MCT4 knockdown resulted in a substantial attenuation of lactate efflux, but glucose uptake persisted. Interestingly, the overexpression of MCT4 in Capan-2 cells resulted in increased lactate efflux, indicating that MCT4 is sufficient to alter lactate transport (Figure S3). We used isotope tracers (^{13}C-glucose) to test whether MCT4 silencing altered the synthesis of lactate from glucose. These data showed that MCT4 knockdown significant impeded the production of new lactate (M+3) from glucose (Figure 4B). To directly measure total intracellular lactate, we employed mass spectrometry (Cheng et al., 2011; Harrison et al., 2012). MCT4 silencing resulted in enhanced lactate retention in MIA PaCa-2 and PL45 cells (Figure 4C), whereas no change was observed in Capan-2 cells (not shown). These data indicate that failure to export lactate leads to an accumulation of intracellular lactate and a corresponding decrease in synthetic rates.

We then used isotope tracers (^{13}C-glucose) to test whether MCT4 silencing altered the labeling of other glucose-dependent metabolic pathways. Analysis of metabolites related to the tricarboxylic acid (TCA) cycle indicated enhanced glucose-dependent labeling (e.g., citrate M+2, aspartate M+2) in MCT4-depleted cells, suggesting a compensatory increase in mitochondrial function (Figure 4D). Consistent with these data, there was an increase in oxidative phosphorylation as measured by the oxygen consumption rate (OCR) with MCT4 knockdown (Figure 4E). One possible source for the additional mitochondrial utilization of glucose-derived carbon is pyruvate carboxylation, which converts pyruvate to oxaloacetate. However, metabolite-labeling patterns that are most indicative of this process (e.g., malate M+3 and citrate M+5) were significantly attenuated via knockdown of MCT4 (Figure 4F). We further evaluated pyruvate carboxylase activity by selectively labeling glucose carbons 3 and 4, and monitoring specific downstream intermediates of pyruvate carboxylation (Figure 4G). The results confirmed that MCT4 knockdown inhibits pyruvate carboxylase-dependent metabolite labeling, suggesting that additional flux through the TCA cycle reflects the additional utilization of glucose-derived acetyl-CoA.

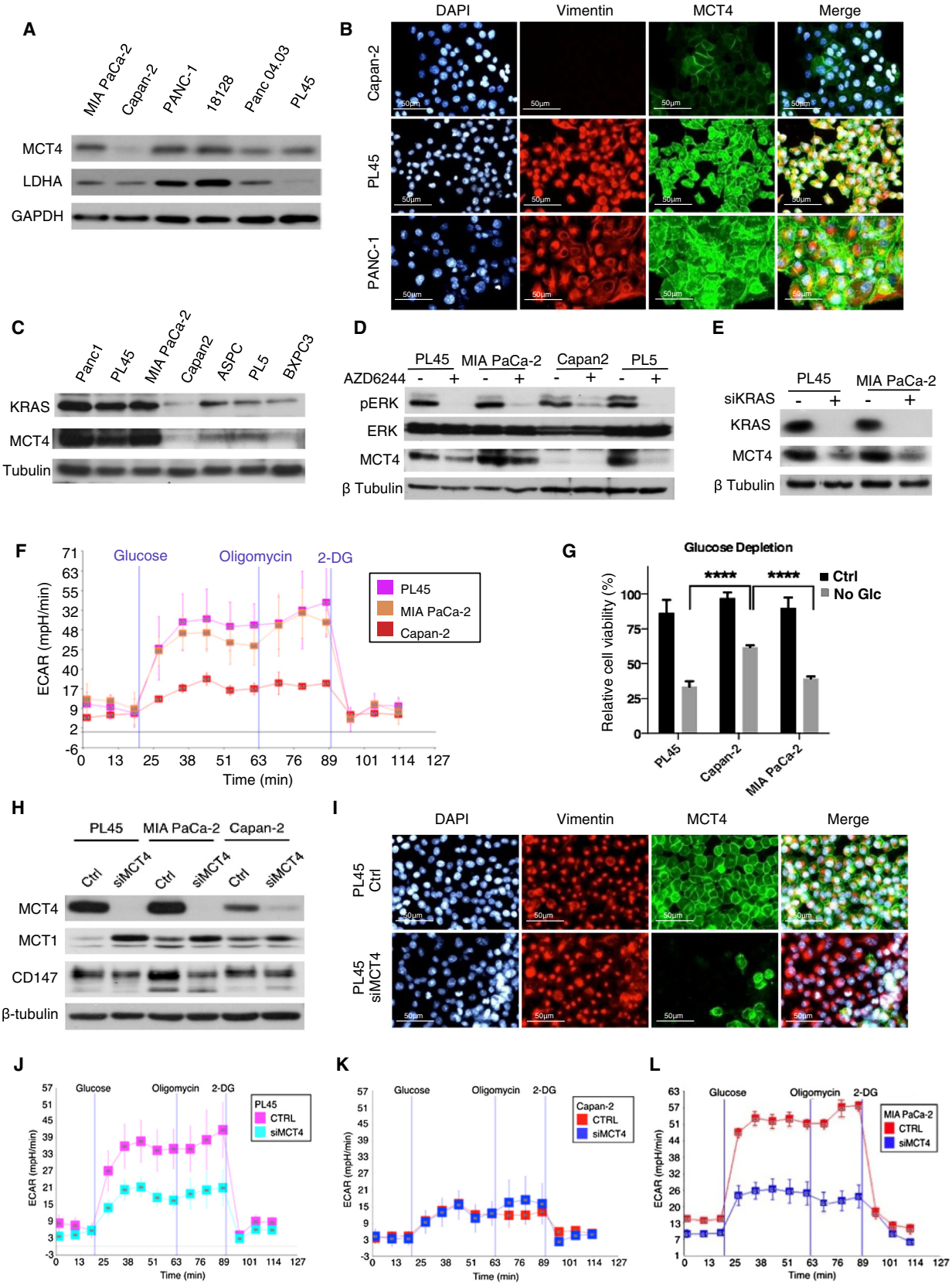

(legend on next page)

Since both glucose and glutamine can be utilized in the TCA cycle, we also evaluated the metabolism of glutamine. Metabolite analysis in the media demonstrated enhanced secretion of glutamate (Figure 4H). Culturing cells with [U-^{13}C] glutamine showed enhanced labeling of TCA cycle intermediates in a pattern indicative of modestly increased contribution of glutamine to anaplerotic pathways, as would be expected in the setting of suppressed pyruvate carboxylation (Cheng et al., 2011; Figure 4I). These data suggest that loss of MCT4 leads to a metabolic crisis, in response to which compensatory mechanisms are rapidly engaged to make up for deficits in glycolysis.

Consistent with these facets of metabolic reprogramming, we observed a significant increase in mitochondrial mass (Figures 5A and 5B) and an increase in reactive oxygen species (ROS) with MCT4 knockdown that could be reversed by pretreatment with antioxidant N-acetylcysteine (NAC; Figure 5C). NAC blocked the HIF1a upregulation observed upon MCT4 knockdown (Figure S4), as previously described (Chandel et al., 1998).

Upregulation of Alternate Metabolic Processes with MCT4 Depletion

In addition to standard pathways for energy production and the genesis of biomolecules, PDA is known to engage in macropinocytosis and autophagy as means of surviving under limited-nutrient conditions (Commisso et al., 2013; Yang and Kimmelman, 2011; Yang et al., 2011). The uptake of fluorescently labeled dextran is the principle means of quantifying macropinocytosis. As shown in Figure 5D, MCT4 knockdown cells showed a significant increase in labeled dextran compared with controls. This could be clearly observed on a per-cell basis in confocal z stacks of the cells (Figure S4). Quantitation of particles on a per-cell basis demonstrated a significant increase in macropinocytosis (Figure 5E). Autophagy was analyzed using LC3 lipidation and the protein levels of p62 (Figure 5F). The results demonstrated a significant increase in lipidated LC3 and corresponding decreased levels of p62, consistent with increased autophagy with MCT4 depletion, and the use of chloroquine confirmed that MCT4 depletion enhanced autophagic flux (Figure S4). Induction of autophagy upon MCT4 knockdown was associated with induction of REDD1, which couples ROS-mediated HIF1a activation to the suppression of mTOR1 signaling and subsequent inhibition of ULK1 phosphorylation (Figure S4). Together, these findings indicate that multiple processes are engaged to compensate for the acute loss of MCT4 in cells that express high levels of the protein, and suggest that MCT4 depletion has a significant impact on cellular fitness.

In order to probe the impact of MCT4 depletion on these disparate adaptive processes, we performed gene-expression profiling. As shown in Figure S4, efficient knockdown was performed in all cell populations with significant alterations in gene expression specific to models with high endogenous levels of MCT4. Selective glycolytic enzymes were downregulated upon knockdown in PL45 and Mia PaCa-2, whereas no change was observed in Capan-2 cells (Figure S4). Correspondingly, Gene Ontology analyses showed that the predominant upregulated genes were significantly associated with blood vessel biogenesis (recognized adaptation to hypoxia) and apoptosis (Figure S4).

MCT4 Depletion Compromises Pancreatic Cancer Cell Survival and Limits Tumorigenic Growth

Morphological analysis of cells with MCT4 knockdown demonstrated an attenuation of cell number and the presence of cells with a refractile appearance (Figure 6A). Flow-cytometric analysis revealed suppression of cell-cycle progression (as determined by bromodeoxyuridine incorporation) and apoptotic cell death (as determined by sub-2N DNA content and Cleaved Caspase-3 immunofluorescence staining) as a consequence of MCT4 knockdown in models that expressed high levels of MCT4 (Figures 6B and 6C). Lastly, analysis of overall viability demonstrated a significant loss of viability that was largely restricted to cell lines with high endogenous expression of MCT4 (Figure 6D) and was not observed with the knockdown of MCT1 (Figure S5). Furthermore, the depletion of CD147 had only a modest effect on cell viability across all models (Figure S5). These data indicate that tumor cells that exhibit high levels of MCT4 are ''addicted'' to this metabolic state, and despite the compensatory mechanisms that are engaged, viability is compromised. In long-term analysis, cells with MCT4 knockdown failed to proliferate, and the resultant cells, which ultimately populated the culture, uniformly regained the expression of MCT4, indicating that there is a key selection for this protein (Figure S5).

To delineate the processes associated with the induction of cell death, we investigated different means of mitigating the proximal effects of MCT4 depletion. First, since lactate synthesis is largely dependent on LDHA, we utilized LDHA knockdown to limit lactate accumulation. As shown in Figure 6E, isolated

Figure 3. MCT4 Expression in Pancreatic Cancer Cell Lines Denotes Glycolytic Metabolism

(A) Levels of MCT4 and LDHA were determined across a panel of pancreatic cancer cell lines. GAPDH served as the control for loading.

(B) The indicated pancreatic cancer cell lines were costained for vimentin and MCT4 expression. Representative images of the staining are shown.

(C) The levels of MCT4 were determined in cell lines with varying KRAS mutation status.

(D) The indicated PDA cell lines were treated with the MEK inhibitor AZD6244 and the indicated proteins were detected by immunoblotting.

(E) The effect of KRAS knockdown on MCT4 protein level was determined by western blot in KRAS-specific, RNAi-transfected Pl45 and MIA PaCa-2 cells.

(F) The indicated PDA cell lines were subjected to a glycolysis stress test with glucose, oligomycin, and 2-DG delivered at the indicated time. ECAR was measured with an XF analyzer.

(G) The indicated PDA cell lines were cultured in the absence of glucose and survival was measured by CellTiter-Glo assay (***$p < 0.001$).

(H and I) The indicated cell populations were transfected with control or MCT4-specific RNAi; immunoblotting (H) and representative fluorescent images (I) are shown.

(J–L) PL45, Capan-2, and MIA PaCa-2 cells transfected with control or MCT4-specific RNAi were subjected to a glycolysis stress test with glucose, oligomycin, and 2-DG delivered at the indicated time. ECAR was measured with an XF analyzer.

See also Figure S3.

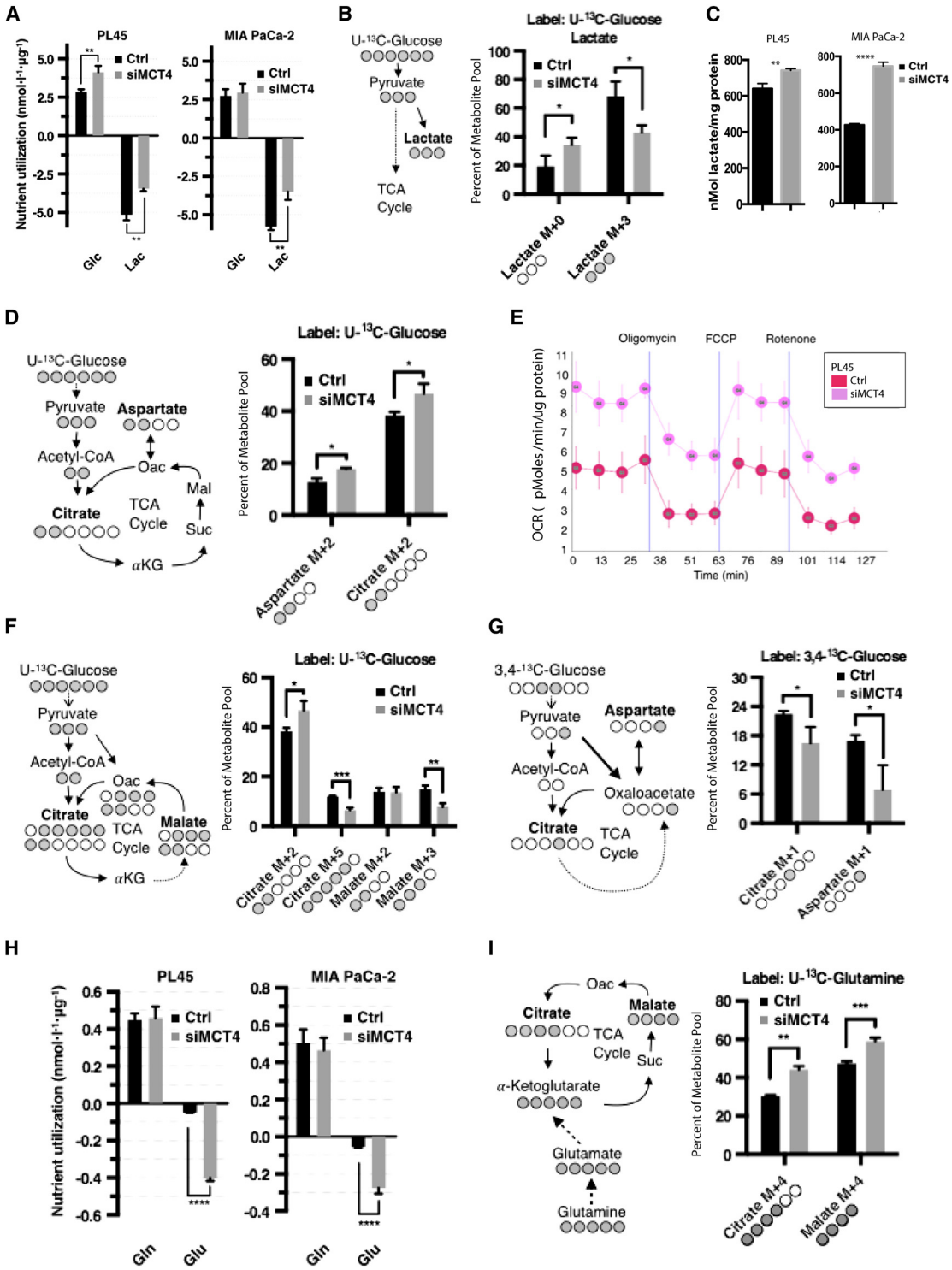

Figure 4. MCT4 Knockdown Leads to Reprogramming of Glucose Metabolism

(A) Medium for nutrient quantitation (DMEM with 10% dialyzed FBS, 20 mM glucose, 4 mM glutamine) was changed at 48 hr posttransfection, and then 0.7 ml of medium was obtained 24 hr later from the indicated cell lines with control or MCT4 knockdown. Concentrations of glucose, lactate, glutamine, and glutamate were determined using an electrochemical analyzer (BioProfile Basic-4 analyzer; NOVA) (**$p < 0.01$). Medium obtained from the indicated cell lines with control or MCT4 knockdown was utilized for the quantitation of glucose consumption and lactate secretion (**$p < 0.01$).

(B) ^{13}C-glucose labeling and liquid chromatography/mass spectrometry (LC/MS) detection were utilized to measure metabolic flux. Analysis of lactate reveals diminished label incorporation with knockdown of MCT4 (*$p < 0.05$).

(legend continued on next page)

LDHA knockdown had a modest effect on cell viability, but could partially rescue the toxicity observed with MCT4 knockdown. Methylpyruvate, a membrane-permeable form of pyruvate, also partially rescued the cell death with MCT4 depletion (Figure 6F). These data suggest that loss of cell viability with MCT4 knockdown is a reflection of metabolic defects associated with lactate accumulation. Interestingly, glucose deprivation neither antagonized nor was additive for MCT4 knockdown, suggesting that the distal mechanisms of those metabolic crises are overlapping (Figure S6). The antioxidant agent NAC inhibited MCT4 knockdown-induced ROS accumulation and rescued cell viability (Figure 6G).

To determine whether the adaptive biological responses of increased mitochondrial metabolism, macropinocytosis, and autophagy were relevant for transient survival with MCT4 depletion, we carried out pharmaceutical challenges relevant to each process (Figures 6H–6J and S6). As shown in Figure 6H, MCT4 knockdown sensitized the cells to further cell killing in combination with the mitochondrial complex 1 inhibitor phenformin. In order to focus specifically on drug effects beyond the impact of MCT4 depletion, we normalized the data to the untreated controls. Consistent with the effects of phenformin, low doses of the complex 1 inhibitor rotenone had a moderate but significant effect on survival that was specific to MCT4-depleted cells (Figure S6). More profound effects were observed with the inhibitors of macropinocytosis (EIPA) and autophagy (chloroquine) (Figures 6I and 6J). Sensitivity to EIPA was specific to cell lines with high levels of endogenous MCT4 (e.g., PL45 and MIA PaCa-2). In contrast, treatment with chloroquine resulted in impaired cell survival in all models. Lastly, to assess the impact of MCT1 inhibition, we treated cells with AR-C155858, which had limited activity as a single agent but cooperated with MCT4 knockdown (Figure S6).

To determine the potential effects of MCT4 on the tumorigenic growth of pancreatic cancer cells, we employed stable short hairpin RNA (shRNA)-mediated knockdown. Lentiviral infection of shRNA limited the expression of MCT4 in pancreatic cancer cell lines (Figures 7A and 7B). Although cells could survive with the residual expression of MCT4, these cell populations grew slowly relative to controls (Figure 7C). To evaluate the effect of MCT4 on tumorigenic growth, we injected parental MIA PaCa-2 and PL45 cells expressing high levels of MCT4 subcutaneously into the left flank of NSG mice, and MIA PaCa-2 shMCT4 and Pl45 shMCT4 cells into the contralateral flank of the same animals. Mice were sacrificed when they became moribund or tumors exceeded 1,000 mm^3. In all cases (n = 14 total), the mice were sacrificed due to the growth of the control MCT4-proficient tumor. Tumors with MCT4 knockdown were smaller as determined by wet weight (Figure 7D) and by visual inspection (Figure 7E). Consistent with the cell culture findings, we observed that reduced MCT4 levels were associated with a lower proliferative index (Ki67) and higher apoptotic index (Cleaved Caspase-3) in the tumor tissues analyzed (Figure S7).

Together, these data indicate that MCT4 plays a critical role in the tumorigenic features of pancreatic cancer and correlate with our observations from clinical cases. To determine how MCT4 knockdown influenced tumor metabolism, we carried out metabolomic profiling on matched tumors (Figure 7F). The data revealed that MCT4 depletion had a profound impact on tumor metabolism (Figure 7G). A metabolomic analysis of tumor tissues showed an increase in lactate levels in shMCT4 tumors, consistent with an inability to excrete this metabolite and similar to previous observations (Schneiderhan et al., 2009). Similarly, depletion of MCT4 was associated with low intratumoral glutamate, consistent with increased export of glutamate into the media with MCT4 depletion in cell culture. shMCT4 tumors displayed low levels of glutathione, consistent with oxidative stress. The high levels of asparagine observed in shMCT4 tumors could be a result of asparagine synthetase activation, which is induced in response to metabolic stress and may protect against decreased intracellular pH (resulting from accumulation of lactate) by providing a source of ammonia (Balasubramanian et al., 2013; Gouzy et al., 2014). Levels of hydroxyphenylpyruvate were increased, possibly indicating that it serves as an energetic substrate for the mitochondrial respiratory chain as well as an antioxidant (Cotoia et al., 2014). Thus, MCT4 depletion reprograms facets of pancreatic cancer metabolism, leading to a deficit in tumorigenic behavior.

DISCUSSION

It is increasingly being recognized that tumor cells exhibit unique metabolic adaptations that influence the biological behavior of the tumor and have prognostic and therapeutic implications (Cheong et al., 2012; White, 2013). Indeed, these properties are collectively now considered an ''emerging hallmark'' of cancer (Cheong et al., 2012; Hanahan and Weinberg, 2011). A well-known example of such an adaptation is the Warburg effect, in which tumor cells exhibit aerobic glycolysis and develop adaptive mechanisms that allow them to survive under acidic

(C) LC/MS was used to determine the intracellular levels of lactate in control or MCT4 knockdown cell lines (**p = 0.02, ****p < 0.0001).
(D) ^{13}C-glucose labeling and LC/MS detection were utilized to measure metabolic flux. Analysis of aspartate and malate revealed enhanced label incorporation with the knockdown of MCT4 (*p < 0.05).
(E) Oxidative metabolism was measured by OCR in the presence of control or MCT4 knockdown.
(F) ^{13}C-glucose and LC/MS were utilized to measure metabolic flux. Analysis of specific labeled metabolites suggested the suppression of pyruvate carboxylate activity (*p < 0.05, **p < 0.01, ***p < 0.001).
(G) Selectively labeled ^{13}C-glucose was used to monitor specific pyruvate carboxylase activity. The data show that attenuation of MCT4 inhibits flux through pyruvate carboxylase (*p < 0.05).
(H) Medium obtained from the indicated cell lines with control or MCT4 knockdown was utilized for the quantitation of glutamine consumption and glutamate efflux (****p < 0.0001).
(I) ^{13}C-glutamine labeling and LC/MS detection were utilized to measure metabolic flux. Analysis of specific metabolites indicated a statistically significant increase in glutamine utilization through the TCA cycle (**p < 0.01, ***p < 0.001).
See also Figure S4.

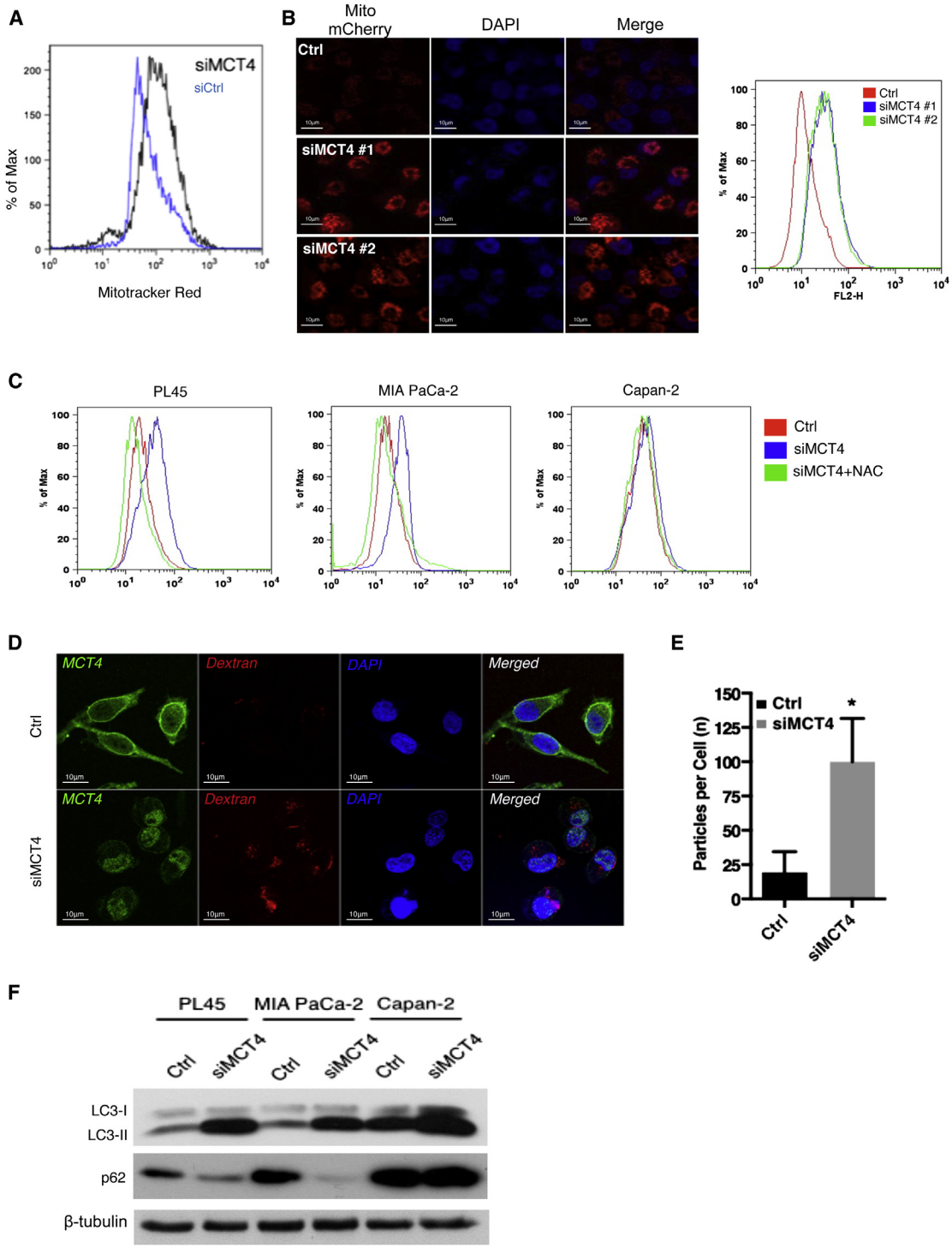

Figure 5. Attenuation of MCT4 Leads to Compensatory Upregulation of Macropinocytosis and Autophagy

(A) Mitochondrial mass was determined by staining with a mitochondrial-specific probe (MitoTracker Red). MitoTracker intensity was measured by flow-cytometric analysis.

(B) Cells were labeled with mitochondrial mCherry. Representative images with two different types of MCT4-specific RNAi are shown. Fluorescence was quantified by flow-cytometric analysis.

(C) Control and MCT4 knockdown cells were treated with a fluorogenic probe to measure ROS. Mean fluorescence intensity represents ROS production.

(legend continued on next page)

conditions (Cheong et al., 2012; Gatenby and Gillies, 2004; Kim and Dang, 2006; Le et al., 2012). Production of lactate is the obligatory byproduct of glycolysis under such conditions, and cancer cells develop several mechanisms that allow them to eliminate excess lactate and survive (Gatenby and Gillies, 2004; Gladden, 2004; Parks et al., 2013). Here, we interrogated a key modulator of lactate homeostasis, MCT4, in the context of PDA.

To date, analysis of PDA has failed to yield specific subtypes that have relevance to treatment of the disease (Tempero et al., 2013). The *Slc16A3* gene is highly expressed in PDA relative to other cancers, and overexpression is a major feature in the transition from normal cells to tumor. The expression of *Slc16A3* is associated with a glycolytic program that is tightly correlated with key enzymes such as hexokinase 2 (HK2), pyruvate kinase 2 (PKM2), and phosphofructo-kinase (PFK). These data suggest that *Slc16A3* is a significant feature of a subtype of pancreatic cancer that is particularly glycolytic. Interestingly, in other tumor types, including Myc-driven Burkitt lymphoma, a subset of breast and lung cancer MCT1 is significantly upregulated and has been shown to correlate with high levels of glycolysis (Birsoy et al., 2013; Doherty et al., 2014; Polański et al., 2014). Surprisingly, *Slc16A3* was also associated with gene expression related to collagen organization. Although the basis for this association is currently under investigation, it suggests an intimate coupling between metabolism and the tumor microenvironment. In general, more aggressive pancreatic cancer cell lines that have progressed through the epithelial to mesenchymal transition express higher levels of MCT4 protein and harbor a glycolytic metabolism. Similarly, clinical PDA cases expressing high levels of MCT4 in the tumor and associated stromal compartments have the worst outcome (median survival: 13.8 months). The regulation and function of stromal MCT4 in this context remain poorly understood. In PDA, the majority of cases that express stromal MCT4 also express high levels of MCT4 in the tumor, suggesting that these events are coupled. Consistent with this point, stromal MCT4 expression is not observed in normal pancreatic tissue or pancreatitis. These data indicate that MCT4 defines a ''metabolic subtype'' of PDA with particularly poor prognosis.

Targeting the unique features of tumor metabolism is increasingly being considered a viable therapeutic strategy. The strong reliance of cancer cells on glucose metabolism yields significant production of lactate. In the absence of mechanisms to export lactate, metabolic feedback mechanisms related to both intracellular pH and the accumulation of intracellular lactate can compromise subsequent production of ATP (Parks et al., 2013). Consistently, high levels of MCT4 correlated with a preference for glycolytic metabolism, and depletion of MCT4 had a significant impact on ECAR. These findings indicate that MCT4 is required for efficient glycolytic metabolism in pancreatic cancer models. Since metabolic networks are complex, with multiple existing compensatory mechanisms, we utilized isotope tracing to determine how MCT4 status affects the utilization of glucose and glutamine. Consistent with the ECAR results, the evidence suggested that MCT4-depleted cells rebalanced the fate of glucose with a shift toward oxidative metabolism. One potential pathway to supply oxidative metabolism is through the action of pyruvate carboxylase, and inherited deficiency of pyruvate carboxylase causes lactic acidosis due to increased pyruvate pools (Jeoung et al., 2014). Interestingly, although cancer cells can utilize pyruvate carboxylase to survive under conditions of glutamine deprivation (Cheng et al., 2011), instead of increasing with MCT4 knockdown, this activity is suppressed, suggesting that pyruvate is being utilized through acetyl-CoA rather than oxaloacetate. Importantly, these data indicate that under conditions of interrupted lactate export by depletion of MCT4, there is a compensatory enhancement of mitochondrial metabolism. In addition to conventional metabolic pathways, macropinocytosis and autophagy have emerged as important sources of metabolites under stress conditions. Interestingly, with the depletion of MCT4, both of these processes were further augmented. This is particularly striking considering that pancreatic cancers models already exhibit ''activated'' levels of these processes (Commisso et al., 2013; Yang and Kimmelman, 2011; Yang et al., 2011). Importantly, these composite data underscore the overall importance of targeting lactate efflux, given the multiple downstream effects on tumor cell metabolism. The idea of targeting tumor metabolism therapeutically has been extensively considered. In general, therapeutic strategies targeting tumor metabolism involve inhibiting a particular nutrient source or metabolic pathway in ''addicted tumors.'' For example, multiple trials are assessing the impact of Lonidamine and TLN232, which target hexokinase and pyruvate kinase, respectively (Tennant et al., 2010). However, given the diverse energy and nutrient sources available to KRAS-driven tumors, these approaches may be challenging (White, 2013). Based on the significant effects on multiple aspects of metabolism, we reasoned that MCT4 depletion targeting ''waste removal'' could represent an important therapeutic target. Although no specific drugs against MCT4 are currently available, acute and stable knockdown had a profound effect on cell survival, inducing apoptotic cell death. This effect was particularly significant for subsets of pancreatic cancer cells that exhibit high levels of the protein and presumably are ''addicted'' to the presence of MCT4. The data presented here provide a rationale for employing selective blockade of MCT4 in a subset of PDA with a particularly poor prognosis. Interestingly, sensitivity to monocarboxylate lactate transporters seems to be an emerging theme, as disruption of another lactate transporter, MCT1, in glycolytic tumors that preferentially express this transporter was shown to lead to an accumulation of intracellular lactate and tumor cell death (Doherty et al., 2014; Polański et al., 2014). Importantly, in contrast to the wide expression of MCT1, MCT4 expression is relatively restricted and thus may provide a potent therapeutic index. However, MCT4 depletion did serve to further sensitize PDA tumor cells to MCT1 inhibitors, suggesting that the ''dual'' blockade of tumor-induced

(D) Cells with control or MCT4 knockdown were exposed to rhodamine-labeled dextran. Uptake of the macromolecules was determined by confocal microscopy.
(E) Dextran particles were quantified from confocal images using ImageJ software (*$p < 0.05$).
(F) Cell lysates were prepared from control or MCT4 knockdown cells as indicated and immunoblotted for p62 and lipidated LC3.
See also Figure S5.

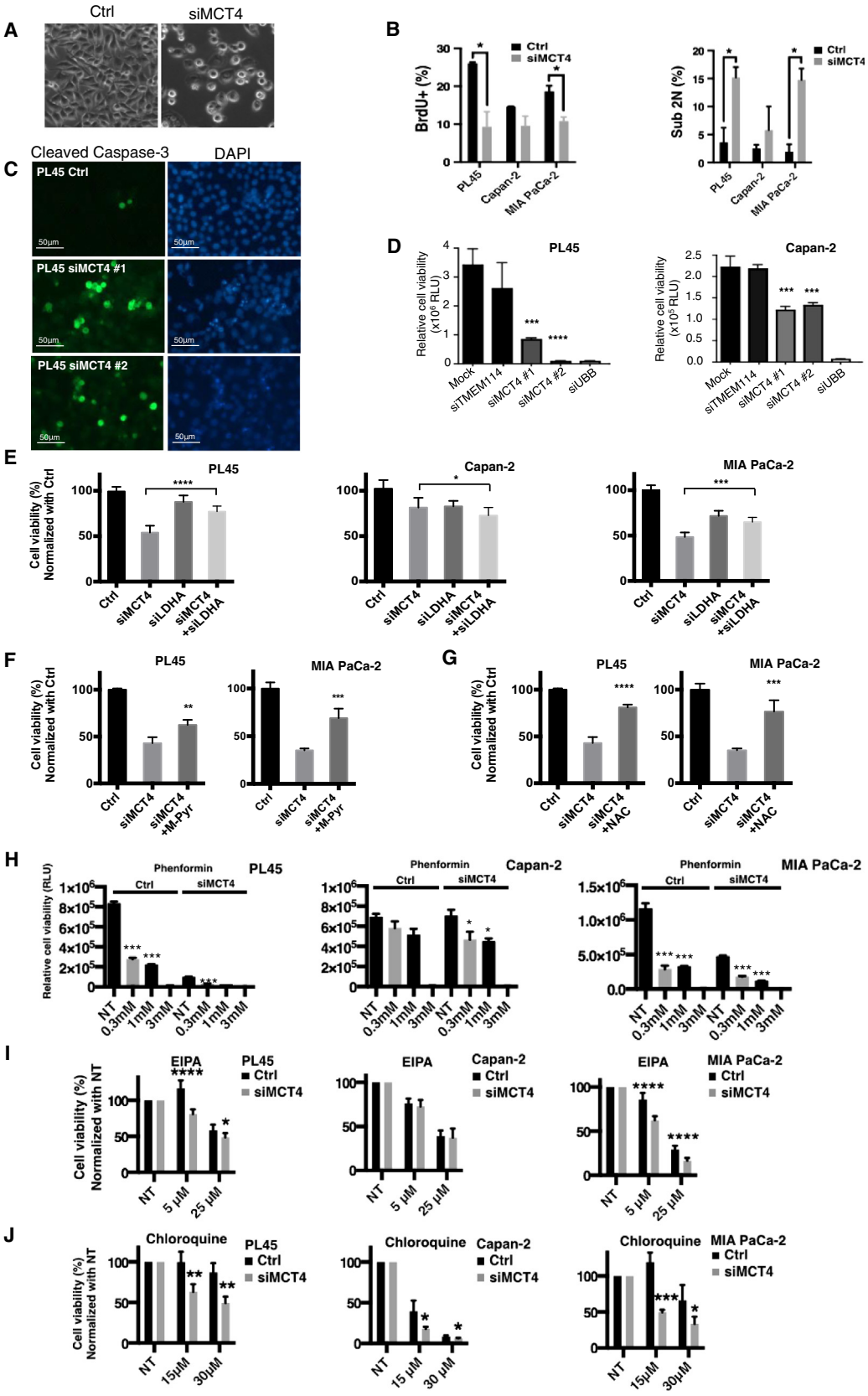

(legend on next page)

lactate transporters could be a viable strategy in specific tumor types. MCT4 depletion was also synergistic with inhibitors of autophagy and macropinocytosis, suggesting that synchronous targeting of multiple compensatory pathways could enhance therapeutic responses.

In this work, we performed a detailed analysis of lactate transporter function and the resultant impact on pancreatic cancer biology. Our data demonstrate that there is substantial diversity in metabolic preference that has not been previously appreciated. This finding was unexpected, given that KRAS mutation occurs in ~95% of PDA and is viewed as being the key driver of metabolic preference, resulting in a relatively monolithic view of the disease and its metabolism. MCT4 status is both associated with and required for glycolytic metabolism with lactate as an endpoint. MCT4 expression is associated with poor prognosis in a cohort of PDA specimens, suggesting that MCT4 is a key marker and determinant of the metabolic state associated with aggressive cancer biology. The data obtained from clinical specimens suggested that only a subset of PDA is addicted/dependent on MCT4 function, and this was confirmed in multiple functional studies. In addicted models, MCT4 depletion has dramatic effects on multiple facets of metabolism. There is an increased utilization of oxidative phosphorylation, with both glucose and glutamine serving as energy sources. Although this would generally be viewed as the default compensatory mechanism, surprisingly, pyruvate carboxylation is inhibited by MCT4 depletion, with most glucose-derived carbon ostensibly coming into the TCA cycle as acetyl-CoA. This compensatory reliance on mitochondrial-based metabolism is associated with production of ROS. The increase in ROS leads to the induction of multiple downstream effector mechanisms, including hypoxia signaling and autophagy. Surprisingly, these adaptations to suppression of MCT4 are not sufficient to rescue apoptotic cell death, although targeting compensatory pathways in concert with MCT4 knockdown augmented cell death via metabolic crisis. Importantly, we show that the metabolic dependence on MCT4 is maintained during tumorigenic growth and has a profound effect on tumor biology. These findings illustrate the metabolic diversity of PDA as described by the presence of MCT4, delineate pathways through which MCT4 supports cancer growth/viability by influencing multiple important metabolic features of disease, and demonstrate that MCT4-high PDA can be rationally targeted based on metabolic addictions.

EXPERIMENTAL PROCEDURES

Cell Culture

The human pancreatic adenocarcinoma lines PL45, Capan-2, MIA PaCa-2, 18128, PANC-1, and Panc 04.03 were cultured under 5% CO_2 at 37°C in Dulbecco's modified Eagle's medium (DMEM; Sigma) supplemented with 10% fetal bovine serum (FBS), penicillin/streptomycin, and 4 mM L-glutamine.

Immunofluorescence and Microscope Imaging

Cells were seeded onto glass coverslips in six-well plates. Staining was performed after cells reached 70%–90% confluence. Cells were washed with PBS, fixed in 3.7% formaldehyde for 15 min at room temperature, permeabilized in 100% methanol for 5 min, and then washed with PBS again. The cells were then blocked in IF buffer (PBS, 0.5% NP40, and 5% BSA) for 10 min at room temperature. Primary antibodies, diluted in IF buffer, were incubated with the cells for 1 hr at room temperature in a humidified chamber. The cells were washed with PBS and then incubated in fluorescent-conjugated secondary antibodies diluted in IF buffer for 30 min at room temperature in a humidified chamber. The cells were again washed three times in PBS, costained with DAPI (in PBS), and mounted onto slides using mounting reagent (ProLong Gold Antifade; Life Technologies). The following antibodies were used: anti-vimentin (mouse monoclonal; Abcam), anti-MCT4 (sc-50329, rabbit polyclonal; Santa Cruz Biotechnology), anti-cleaved caspase3 (D175, rabbit polyclonal; Cell Signaling Technology), anti-rabbit Alexa Fluor 488 conjugated immunoglobulin G (Life Technologies), and anti-rabbit Alexa Fluor 546 conjugated immunoglobulin G (Life Technologies). Images were captured using a Zeiss fluorescent microscope (Zeiss).

Measurement of ECAR and OCR

Cells were seeded into an XF assay microplate (Seahorse Bioscience) 1 day before the day of assay. The assay cartridge was hydrated overnight at 37°C in a CO_2-free incubator. On the day of assay, the growth medium was changed with assay medium (DMEM with 1.85 g/L NaCl, 3 mg/L phenol red, 2 mM L-glutamine). Glucose, oligomycin, and 2-DG for ECAR, and oligomycine, FCCP, and rotenone for OCR were sequentially injected into each well in accordance with the manufacturer's standard protocol. The resultant alterations in pH and mitochondrial respiration were measured by the sensor probe on an XF24 extracellular flux analyzer (Seahorse Bioscience). Results were normalized to the protein content of each well.

Nutrient Utilization and Secretion

Cells were seeded in six-well plates and 1 ml of medium was collected from each well in triplicate. Concentrations of glucose, lactate, glutamine, and glutamate were determined using an automated electrochemical analyzer (BioProfile Basic-4 Analyzer; NOVA). Metabolic concentrations were normalized by protein content using the BCA Protein Assay (Bio-Rad).

Microarray Analysis

Cells were transfected with either control or MCT4-selective RNAi. Cells were harvested and total RNA was harvested using standard methods. RNA was

Figure 6. MCT4 Is Required for the Viability of PDA Cells with High Endogenous Levels

(A) Representative phase-contrast images of PL45 cells with control or MCT4 knockdown.

(B) Flow-cytometry analysis of bromodeoxyuridine incorporation (left panel) and sub-2N DNA content (right panel).

(C) Immunofluorescence staining for Cleaved Caspase-3 from PL45 cells with control or two different MCT4 knockdowns. Representative images are shown.

(D) Analysis of cell viability by Cell-Titer Glow analysis from the indicated cells transfected with TMEM RNAi (negative control), two different types of MCT4 RNAi, and UBB RNAi (positive control).

(E) Cells were transfected with MCT4-specific or LDHA-specific RNAi. Cell viability was determined by Cell-Titer Glow analysis.

(F) Cells were transfected with MCT4-specific RNAi and cotreated with 4 mM of methyl pyruvate for 48 hr. Cell viability was determined by Cell-Titer Glow analysis.

(G) Cells were transfected with MCT4-specific RNAi and cotreated with 2 mM of NAC for 48 hr. Cell viability was determined by Cell-Titer Glow analysis.

(H) Cells transfected with control or MCT4-specific RNAi were exposed to phenformin, inhibiting mitochondrial function. Cell viability was determined by Cell-Titer Glow analysis.

(I and J) Cells transfected with control or MCT4-specific RNAi were exposed to agents that inhibit macropinocytosis (EIPA) or autophagy (chloroquine). The normalized impact of the agents on survival is plotted (*$p < 0.05$, **$p < 0.01$, ***$p < 0.001$, ****$p < 0.0001$).

See also Figure S6.

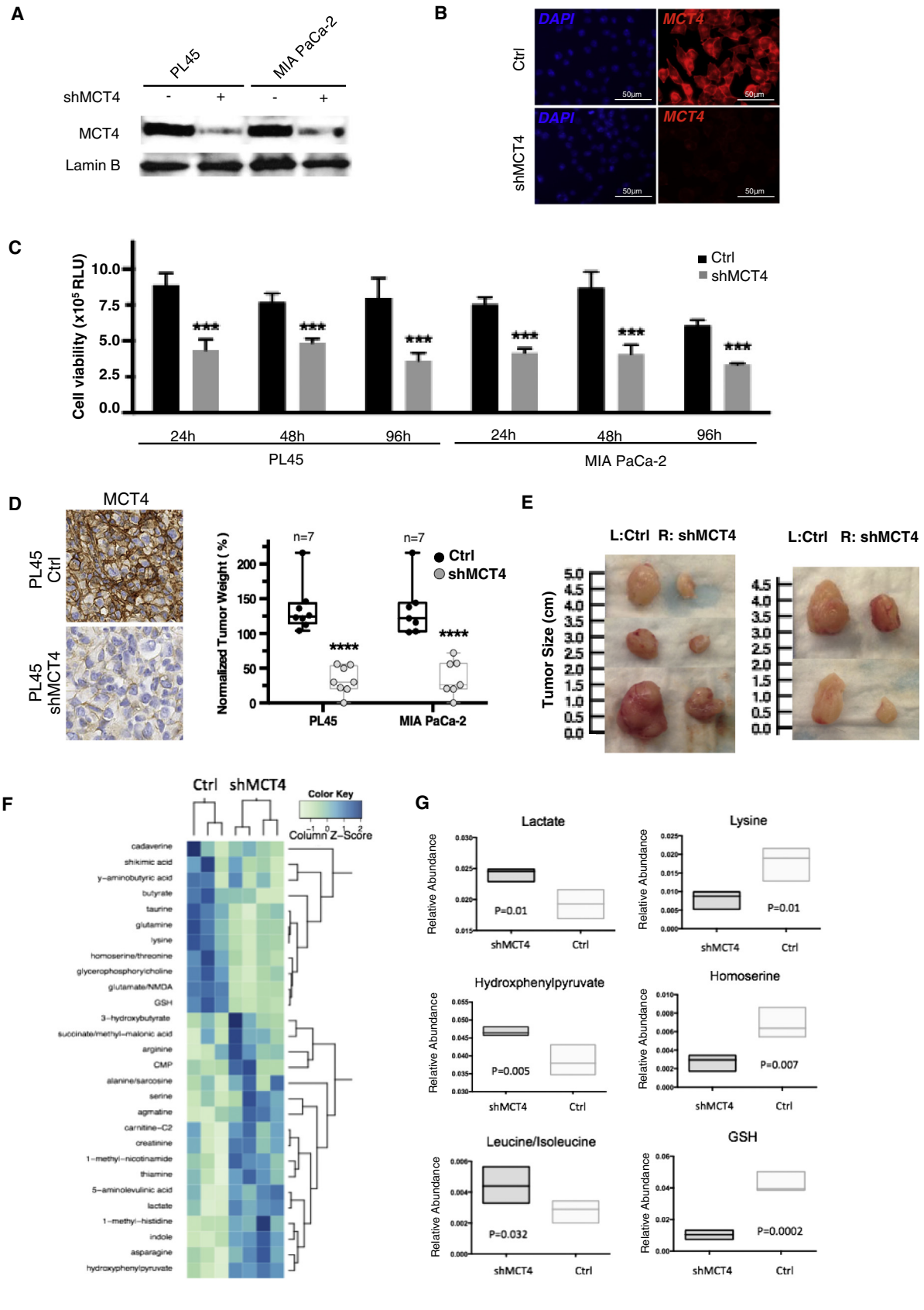

(legend on next page)

hybridized on Agilent gene array platforms and differential expression of robust multiarray average (RMA) normalized data is provided.

Metabolic Tracing Using ^{13}C Stable Isotopes

For analysis of intracellular metabolites by gas chromatography/mass spectrometry, 80%–90% confluent cells in 60 mm dishes were washed twice with PBS, incubated in medium containing ^{13}C isotopically enriched nutrient ([U-$^{13}C6$] D-glucose, [U-$^{13}C5$] L-glutamine, [3,4-$^{13}C2$] D-glucose; Cambridge Isotope Laboratories), and cultured for 7 hr. Unless otherwise indicated, cells for metabolic experiments were used 72 hr after control and siMCT4 RNA transfection. Isotope-labeled cells were washed twice with cold PBS and lysed with three freeze-thaw cycles in 50% ice-cold methanol and 50% water. The lysates were centrifuged to remove precipitated protein, a standard (50 nmol of sodium 2-oxobutyrate) was added, and the samples were evaporated and derivatized by trimethylsilylation (Tri-Sil HTP reagent; Thermo Scientific). Three microliters of the derivatized material was injected into an Agilent 6970 gas chromatograph equipped with a fused silica capillary GC column (30 m long, 0.25 mm in diameter) and networked to an Agilent 5973 mass selective detector. The retention times of all of the metabolites were validated using pure standards. The abundance of the following ions was monitored: m/z 465-471 for citrate, m/z 334-338 for aspartate, m/z 335-339 for malate, and m/z 219-222 for lactate. The measured distribution of mass isotopomers was corrected mathematically for natural abundance of ^{13}C and represented as a percentage of the total pool. To measure the intracellular lactate pool, an isotopic standard of lactate was used as described previously (Harrison et al., 2012).

Tumor Microarray Construction and Population Study

Cases for the study were obtained from the surgical pathology files at Thomas Jefferson University with Institutional Review Board approval. All animal studies were performed in accordance with the IACUC guidelines of UT Southwestern. The tissue microarray (TMA) contained tumor samples derived from 223 largely consecutive patients with PDA who had been treated at Thomas Jefferson University Hospitals between the years 2002 and 2010. Prior to TMA construction, hematoxylin and eosin (H&E) tumor sections from each case were reviewed and representative areas of PDA were selected. Each case was represented in the TMA by two cores (6 mm diameter) and deposited into a recipient paraffin block with the use of a TMA workstation (TMA builder, Veridiam). Tissue sections (4 μm) were used for immunohistochemistry and an H&E-stained section from each TMA block was reviewed to confirm the presence of morphologically representative areas of the original tissues. Clinical and treatment information was extracted by chart review.

Immunohistochemistry

Immunohistochemistry was performed as previously described (Witkiewicz et al., 2012). In brief, MCT1 and MCT4 expression levels were assessed using a standard avidin-biotin immunoperoxidase method with a rabbit polyclonal anti-MCT1 (developed and characterized by Dr. Nancy Philp [Gallagher et al., 2007]; 1:250) and MCT4 antibodies (developed and characterized by Dr. Nancy Philp [Gallagher et al., 2007]; 1:250). TMA sections were deparaffinized and rehydrated through graded alcohols. Antigen retrieval was performed in 10 nM citrate buffer (pH 6.0) for 10 min in a pressure cooker. Sections were cooled to room temperature, rinsed in PBS, blocked with 3% (v/v) H_2O_2 for 15 min, and then blocked for endogenous biotin using the Dako Cytomation Biotin Blocking System (Dako). Slides were then incubated for 1 hr with 10% goat serum and incubated with primary antibody overnight at 4°C. Antibody binding was detected using a biotinylated secondary antibody (Vector Labs) followed by streptavidin horseradish peroxidase (Dako). Immunoreactivity was detected using 3,3′ diaminobenzidine.

Statistical Analysis

Data analyses were conducted in GraphPad Prism software. Stromal MCT4 expression in the TMAs was scored as 0 (none), 1 (weak), or 2 (strong). Epithelial MCT4 and MCT1 were scored as 0 (none), 1–4 (weak), or 6–9 (strong). Survival curves were computed by expression strata using the Kaplan-Meier method, and differences between overall survival curves was assessed using the log rank test. Hazard ratios for the biomarkers were computed using Cox proportional hazards regression, using the biomarker as predictor. For the statistical analysis of molecular data, the following convention was utilized: *$p < 0.05$, **$p < 0.01$, ***$p < 0.001$, ****$p < 0.0001$.

For additional details regarding the materials and methods used in this work, see Supplemental Experimental Procedures.

ACCESSION NUMBERS

The NCBI Gene Expression Omnibus accession number for the data reported in this paper is GSE63231.

SUPPLEMENTAL INFORMATION

Supplemental Information includes Supplemental Experimental Procedures, seven figures, and two tables and can be found with this article online at http://dx.doi.org/10.1016/j.celrep.2014.11.025.

ACKNOWLEDGMENTS

The authors thank all of the members of the A.K.W. laboratory and colleagues for helpful discussions, editorial advice, and reagents. Dr. Nicholas Borja assisted with editorial comments, Ms Uthra Balaji assisted with the informatics, and Dr. Thomas Pajak assisted with the statistics. Training grant support for G.H.B. was provided by the Cancer Prevention Research Institute of Texas (CPRIT RP140110). M.A.W. received funding from the Welch Foundation (I-1414).

Received: October 3, 2014
Revised: November 4, 2014
Accepted: November 17, 2014
Published: December 11, 2014

REFERENCES

Almhanna, K., and Philip, P.A. (2011). Defining new paradigms for the treatment of pancreatic cancer. Curr. Treat. Options Oncol. *12*, 111–125.

Balasubramanian, M.N., Butterworth, E.A., and Kilberg, M.S. (2013). Asparagine synthetase: regulation by cell stress and involvement in tumor biology. Am. J. Physiol. Endocrinol. Metab. *304*, E789–E799.

Bardeesy, N., and DePinho, R.A. (2002). Pancreatic cancer biology and genetics. Nat. Rev. Cancer *2*, 897–909.

Bergersen, L.H. (2007). Is lactate food for neurons? Comparison of monocarboxylate transporter subtypes in brain and muscle. Neuroscience *145*, 11–19.

Figure 7. MCT4 Fuels the Growth of PDA Tumors

(A and B) shRNA-mediated knockdown of MCT4 was confirmed in the indicated cell lines by immunoblot and immunofluorescence analysis.

(C) shRNA-mediated knockdown of MCT4 resulted in attenuated proliferative capacity as shown by Cell-Titer Glow analysis (***$p < 0.001$).

(D and E) Equal amounts of control and MCT4 knockdown cells were injected contralaterally into NSG mice. Mice were aged until their tumors reached ~1,500 mm^3 or the mice became moribund. Depletion of MCT4 was confirmed by immunohistochemical staining, and the relative wet weight and size of the tumors are shown.

(F and G) Metabolomic profiling of xenograft tumors indicates an alteration in metabolite levels between control and knockdown tumors. The relative abundance of selected metabolites from the tumors analyzed is shown in arbitrary units.

See also Figure S7.

Bergersen, L., Jóhannsson, E., Veruki, M.L., Nagelhus, E.A., Halestrap, A., Sejersted, O.M., and Ottersen, O.P. (1999). Cellular and subcellular expression of monocarboxylate transporters in the pigment epithelium and retina of the rat. Neuroscience *90*, 319–331.

Birsoy, K., Wang, T., Possemato, R., Yilmaz, O.H., Koch, C.E., Chen, W.W., Hutchins, A.W., Gultekin, Y., Peterson, T.R., Carette, J.E., et al. (2013). MCT1-mediated transport of a toxic molecule is an effective strategy for targeting glycolytic tumors. Nat. Genet. *45*, 104–108.

Bonen, A. (2000). Lactate transporters (MCT proteins) in heart and skeletal muscles. Med. Sci. Sports Exerc. *32*, 778–789.

Brahimi-Horn, M.C., Bellot, G., and Pouysségur, J. (2011). Hypoxia and energetic tumour metabolism. Curr. Opin. Genet. Dev. *21*, 67–72.

Chandel, N.S., Maltepe, E., Goldwasser, E., Mathieu, C.E., Simon, M.C., and Schumacker, P.T. (1998). Mitochondrial reactive oxygen species trigger hypoxia-induced transcription. Proc. Natl. Acad. Sci. USA *95*, 11715–11720.

Cheng, T., Sudderth, J., Yang, C., Mullen, A.R., Jin, E.S., Matés, J.M., and DeBerardinis, R.J. (2011). Pyruvate carboxylase is required for glutamine-independent growth of tumor cells. Proc. Natl. Acad. Sci. USA *108*, 8674–8679.

Cheong, H., Lu, C., Lindsten, T., and Thompson, C.B. (2012). Therapeutic targets in cancer cell metabolism and autophagy. Nat. Biotechnol. *30*, 671–678.

Chu, G.C., Kimmelman, A.C., Hezel, A.F., and DePinho, R.A. (2007). Stromal biology of pancreatic cancer. J. Cell. Biochem. *101*, 887–907.

Commisso, C., Davidson, S.M., Soydaner-Azeloglu, R.G., Parker, S.J., Kamphorst, J.J., Hackett, S., Grabocka, E., Nofal, M., Drebin, J.A., Thompson, C.B., et al. (2013). Macropinocytosis of protein is an amino acid supply route in Ras-transformed cells. Nature *497*, 633–637.

Cotoia, A., Scrima, R., Gefter, J.V., Piccoli, C., Cinnella, G., Dambrosio, M., Fink, M.P., and Capitanio, N. (2014). p-Hydroxyphenylpyruvate, an intermediate of the Phe/Tyr catabolism, improves mitochondrial oxidative metabolism under stressing conditions and prolongs survival in rats subjected to profound hemorrhagic shock. PLoS ONE *9*, e90917.

Deberardinis, R.J., Sayed, N., Ditsworth, D., and Thompson, C.B. (2008). Brick by brick: metabolism and tumor cell growth. Curr. Opin. Genet. Dev. *18*, 54–61.

Doherty, J.R., Yang, C., Scott, K.E., Cameron, M.D., Fallahi, M., Li, W., Hall, M.A., Amelio, A.L., Mishra, J.K., Li, F., et al. (2014). Blocking lactate export by inhibiting the Myc target MCT1 Disables glycolysis and glutathione synthesis. Cancer Res. *74*, 908–920.

Draoui, N., and Feron, O. (2011). Lactate shuttles at a glance: from physiological paradigms to anti-cancer treatments. Dis. Model. Mech. *4*, 727–732.

Draoui, N., Schicke, O., Seront, E., Bouzin, C., Sonveaux, P., Riant, O., and Feron, O. (2014). Antitumor activity of 7-aminocarboxycoumarin derivatives, a new class of potent inhibitors of lactate influx but not efflux. Mol. Cancer Ther. *13*, 1410–1418.

Erkan, M., Hausmann, S., Michalski, C.W., Fingerle, A.A., Dobritz, M., Kleeff, J., and Friess, H. (2012). The role of stroma in pancreatic cancer: diagnostic and therapeutic implications. Nat Rev Gastroenterol Hepatol *9*, 454–467.

Gallagher, S.M., Castorino, J.J., Wang, D., and Philp, N.J. (2007). Monocarboxylate transporter 4 regulates maturation and trafficking of CD147 to the plasma membrane in the metastatic breast cancer cell line MDA-MB-231. Cancer Res. *67*, 4182–4189.

Gatenby, R.A., and Gillies, R.J. (2004). Why do cancers have high aerobic glycolysis? Nat. Rev. Cancer *4*, 891–899.

Gerlinger, M., Santos, C.R., Spencer-Dene, B., Martinez, P., Endesfelder, D., Burrell, R.A., Vetter, M., Jiang, M., Saunders, R.E., Kelly, G., et al. (2012). Genome-wide RNA interference analysis of renal carcinoma survival regulators identifies MCT4 as a Warburg effect metabolic target. J. Pathol. *227*, 146–156.

Gladden, L.B. (2004). Lactate metabolism: a new paradigm for the third millennium. J. Physiol. *558*, 5–30.

Gouzy, A., Larrouy-Maumus, G., Bottai, D., Levillain, F., Dumas, A., Wallach, J.B., Caire-Brandli, I., de Chastellier, C., Wu, T.D., Poincloux, R., et al. (2014). Mycobacterium tuberculosis exploits asparagine to assimilate nitrogen and resist acid stress during infection. PLoS Pathog. *10*, e1003928.

Halestrap, A.P. (2012). The monocarboxylate transporter family—Structure and functional characterization. IUBMB Life *64*, 1–9.

Halestrap, A.P., and Meredith, D. (2004). The SLC16 gene family-from monocarboxylate transporters (MCTs) to aromatic amino acid transporters and beyond. Pflugers Arch. *447*, 619–628.

Halestrap, A.P., and Price, N.T. (1999). The proton-linked monocarboxylate transporter (MCT) family: structure, function and regulation. Biochem. J. *343*, 281–299.

Halestrap, A.P., and Wilson, M.C. (2012). The monocarboxylate transporter family—role and regulation. IUBMB Life *64*, 109–119.

Hanahan, D., and Weinberg, R.A. (2011). Hallmarks of cancer: the next generation. Cell *144*, 646–674.

Harrison, C., Yang, C., Jindal, A., DeBerardinis, R.J., Hooshyar, M.A., Merritt, M., Dean Sherry, A., and Malloy, C.R. (2012). Comparison of kinetic models for analysis of pyruvate-to-lactate exchange by hyperpolarized 13 C NMR. NMR Biomed. *25*, 1286–1294.

Hezel, A.F., Kimmelman, A.C., Stanger, B.Z., Bardeesy, N., and Depinho, R.A. (2006). Genetics and biology of pancreatic ductal adenocarcinoma. Genes Dev. *20*, 1218–1249.

Ide, T., Kitajima, Y., Miyoshi, A., Ohtsuka, T., Mitsuno, M., Ohtaka, K., and Miyazaki, K. (2007). The hypoxic environment in tumor-stromal cells accelerates pancreatic cancer progression via the activation of paracrine hepatocyte growth factor/c-Met signaling. Ann. Surg. Oncol. *14*, 2600–2607.

Jeoung, N.H., Harris, C.R., and Harris, R.A. (2014). Regulation of pyruvate metabolism in metabolic-related diseases. Rev. Endocr. Metab. Disord. *15*, 99–110.

Kim, J.W., and Dang, C.V. (2006). Cancer's molecular sweet tooth and the Warburg effect. Cancer Res. *66*, 8927–8930.

Kirk, P., Wilson, M.C., Heddle, C., Brown, M.H., Barclay, A.N., and Halestrap, A.P. (2000). CD147 is tightly associated with lactate transporters MCT1 and MCT4 and facilitates their cell surface expression. EMBO J. *19*, 3896–3904.

Le, A., Rajeshkumar, N.V., Maitra, A., and Dang, C.V. (2012). Conceptual framework for cutting the pancreatic cancer fuel supply. Clin. Cancer Res. *18*, 4285–4290.

Le Floch, R., Chiche, J., Marchiq, I., Naiken, T., Ilc, K., Murray, C.M., Critchlow, S.E., Roux, D., Simon, M.P., and Pouysségur, J. (2011). CD147 subunit of lactate/H+ symporters MCT1 and hypoxia-inducible MCT4 is critical for energetics and growth of glycolytic tumors. Proc. Natl. Acad. Sci. USA *108*, 16663–16668.

Lee, I., Lee, S.J., Kang, W.K., and Park, C. (2012). Inhibition of monocarboxylate transporter 2 induces senescence-associated mitochondrial dysfunction and suppresses progression of colorectal malignancies in vivo. Mol. Cancer Ther. *11*, 2342–2351.

Neesse, A., Michl, P., Frese, K.K., Feig, C., Cook, N., Jacobetz, M.A., Lolkema, M.P., Buchholz, M., Olive, K.P., Gress, T.M., and Tuveson, D.A. (2011). Stromal biology and therapy in pancreatic cancer. Gut *60*, 861–868.

Parks, S.K., Chiche, J., and Pouysségur, J. (2013). Disrupting proton dynamics and energy metabolism for cancer therapy. Nat. Rev. Cancer *13*, 611–623.

Philp, N.J., Yoon, H., and Lombardi, L. (2001). Mouse MCT3 gene is expressed preferentially in retinal pigment and choroid plexus epithelia. Am. J. Physiol. Cell Physiol. *280*, C1319–C1326.

Pinheiro, C., Longatto-Filho, A., Scapulatempo, C., Ferreira, L., Martins, S., Pellerin, L., Rodrigues, M., Alves, V.A., Schmitt, F., and Baltazar, F. (2008). Increased expression of monocarboxylate transporters 1, 2, and 4 in colorectal carcinomas. Virchows Arch. *452*, 139–146.

Pinheiro, C., Reis, R.M., Ricardo, S., Longatto-Filho, A., Schmitt, F., and Baltazar, F. (2010). Expression of monocarboxylate transporters 1, 2, and 4 in human tumours and their association with CD147 and CD44. J. Biomed. Biotechnol. *2010*, 427694.

Pinheiro, C., Longatto-Filho, A., Azevedo-Silva, J., Casal, M., Schmitt, F.C., and Baltazar, F. (2012). Role of monocarboxylate transporters in human cancers: state of the art. J. Bioenerg. Biomembr. *44*, 127–139.

Polański, R., Hodgkinson, C.L., Fusi, A., Nonaka, D., Priest, L., Kelly, P., Trapani, F., Bishop, P.W., White, A., Critchlow, S.E., et al. (2014). Activity of the monocarboxylate transporter 1 inhibitor AZD3965 in small cell lung cancer. Clin. Cancer Res. *20*, 926–937.

Schneiderhan, W., Scheler, M., Holzmann, K.H., Marx, M., Gschwend, J.E., Bucholz, M., Gress, T.M., Seufferlein, T., Adler, G., and Oswald, F. (2009). CD147 silencing inhibits lactate transport and reduces malignant potential of pancreatic cancer cells in in vivo and in vitro models. Gut *58*, 1391–1398.

Son, J., Lyssiotis, C.A., Ying, H., Wang, X., Hua, S., Ligorio, M., Perera, R.M., Ferrone, C.R., Mullarky, E., Shyh-Chang, N., et al. (2013). Glutamine supports pancreatic cancer growth through a KRAS-regulated metabolic pathway. Nature *496*, 101–105.

Sonveaux, P., Copetti, T., De Saedeleer, C.J., Végran, F., Verrax, J., Kennedy, K.M., Moon, E.J., Dhup, S., Danhier, P., Frérart, F., et al. (2012). Targeting the lactate transporter MCT1 in endothelial cells inhibits lactate-induced HIF-1 activation and tumor angiogenesis. PLoS ONE *7*, e33418.

Su, J., Chen, X., and Kanekura, T. (2009). A CD147-targeting siRNA inhibits the proliferation, invasiveness, and VEGF production of human malignant melanoma cells by down-regulating glycolysis. Cancer Lett. *273*, 140–147.

Tempero, M.A., Klimstra, D., Berlin, J., Hollingsworth, T., Kim, P., Merchant, N., Moore, M., Pleskow, D., Wang-Gillam, A., and Lowy, A.M. (2013). Changing the way we do business: recommendations to accelerate biomarker development in pancreatic cancer. Clin. Cancer Res. *19*, 538–540.

Tennant, D.A., Durán, R.V., and Gottlieb, E. (2010). Targeting metabolic transformation for cancer therapy. Nat. Rev. Cancer *10*, 267–277.

Whitaker-Menezes, D., Martinez-Outschoorn, U.E., Lin, Z., Ertel, A., Flomenberg, N., Witkiewicz, A.K., Birbe, R.C., Howell, A., Pavlides, S., Gandara, R., et al. (2011). Evidence for a stromal-epithelial "lactate shuttle" in human tumors: MCT4 is a marker of oxidative stress in cancer-associated fibroblasts. Cell Cycle *10*, 1772–1783.

White, E. (2013). Exploiting the bad eating habits of Ras-driven cancers. Genes Dev. *27*, 2065–2071.

Witkiewicz, A.K., Whitaker-Menezes, D., Dasgupta, A., Philp, N.J., Lin, Z., Gandara, R., Sneddon, S., Martinez-Outschoorn, U.E., Sotgia, F., and Lisanti, M.P. (2012). Using the "reverse Warburg effect" to identify high-risk breast cancer patients: stromal MCT4 predicts poor clinical outcome in triple-negative breast cancers. Cell Cycle *11*, 1108–1117.

Wolfgang, C.L., Herman, J.M., Laheru, D.A., Klein, A.P., Erdek, M.A., Fishman, E.K., and Hruban, R.H. (2013). Recent progress in pancreatic cancer. CA Cancer J. Clin. *63*, 318–348.

Wood, L.D., and Hruban, R.H. (2012). Pathology and molecular genetics of pancreatic neoplasms. Cancer J. *18*, 492–501.

Yang, S., and Kimmelman, A.C. (2011). A critical role for autophagy in pancreatic cancer. Autophagy *7*, 912–913.

Yang, S., Wang, X., Contino, G., Liesa, M., Sahin, E., Ying, H., Bause, A., Li, Y., Stommel, J.M., Dell'antonio, G., et al. (2011). Pancreatic cancers require autophagy for tumor growth. Genes Dev. *25*, 717–729.